1. Ravee PHROMLOUNGSRI [1], 2. Mitchai CHONGCHEAWCHAMNAN [2] 3. Somchat SONASANG [3*]

Udon Thani Rajabhat University (1), Prince of Songkla University (2), Nakhon Phanom University (3)
ORCID: 1. https://orcid.org/0000-0002-3614-3404; 2. https://orcid.org/0000-0002-3243-9646 ; 3. https://orcid.org/0000-0002-3261-4547

doi:10.15199/48.2023.10.11

Inductively Compensated Coupled-Line Resonator and Its Bandpass Filter Applications

Abstract. *A compact resonator with inductively compensated coupled lines is proposed. The resonator is achieved by applying an inductive compensation technique to miniaturize quarter-wave coupled lines. The theory and equivalent circuit of the resonator are developed, and design closed-form equations are derived. To demonstrate the application of the resonator, a 1.57 GHz bandpass filter with a 5% fractional bandwidth is designed and fabricated. The experimental results show good agreement with the electromagnetic simulation results. The measured in-band insertion (S_{21}) and return losses (S_{11}) are less than 1.20 dB and 23.20 dB, respectively.*

Streszczenie. *Zaproponowano kompaktowy rezonator z kompensowanymi indukcyjnie liniami sprzężonymi. Rezonator uzyskuje się poprzez zastosowanie techniki kompensacji indukcyjnej w celu miniaturyzacji sprzężonych linii ćwierćfalowych. Opracowano teorię i równoważny obwód rezonatora oraz wyprowadzono równania projektowe w postaci zamkniętej. Aby zademonstrować zastosowanie rezonatora, zaprojektowano i wykonano filtr pasmowoprzepustowy 1,57 GHz z ułamkową szerokością pasma wynoszącą 5%. Wyniki eksperymentalne wykazują dobrą zgodność z wynikami symulacji elektromagnetycznej. Zmierzone straty wtrąceniowe (S_{21}) i odbiciowe (S_{11}) w paśmie są mniejsze niż odpowiednio 1,20 dB i 23,20 dB. (**Rezonator sprzężonej linii z kompensacją indukcyjną i jego zastosowania w filtrach pasmowoprzepustowych**)*

Keywords: Microstrip bandpass filter, octadic-wavelength parallel coupled lines.
Słowa kluczowe: Mikropaskowy filtr pasmowoprzepustowy, równoległe linie sprzężone o długości fali oktadowej.

Introduction

A compact planar narrowband bandpass filter (BPF) is required for several communication applications, such as aircraft surveillance, global positioning, mobile services, and digital audio broadcasting. Especially in current communication situations where several wireless channels are used, a sharp-cutoff, low-loss and high out-of-band rejection BPF design is required [1]. It is well known that the performance of BPFs implemented with lumped capacitors and inductors at microwave and millimeter waves is poor due to the effect of parasitic elements inherent in the lump elements. This considerably deteriorates performance, including insertion loss, input/output matching, and attenuation slope. A BPF realization scheme with transmission lines proposed to circumvent the parasitic effect was demonstrated at high-frequency bands. However, the circuit size of the designs based on a transmission line is not compact because the resonator is based on a quarter-wavelength structure. For these reasons, several microwave and millimeter-wave BPFs with quarter-wave structures have a bulky design [2-5].

Traditionally, planar transmission-line BPFs have been designed with quarter-wave parallel coupled lines, coupled-line stub, and transmission line stubs [6]. A BPF designed with coupled lines or coupled lines stubs demonstrate spurious responses at the out-of-band and consumes circuit area [7]. A quarter-wave (λ/4) coupled-line resonator is one of the most used transmission-line resonators for microwave and millimeter-wave applications due to its simple design flow [8,9]. When a planar BPF is needed, a parallel coupled-line resonator is usually chosen due to its simple structure and available closed-form design equations. It is commonly found that microstrip coupled lines have low directivity, and the frequency response of a microstrip coupled-line BPF contains spurious responses at every even harmonic because the odd-mode wave travels faster than the even-mode wave in inhomogeneous media. Another major limitation is the weak coupling due to lateral coupling between the lines in inhomogeneous media of microstrip coupled lines. These limitations can be overcome by either providing different line lengths for even- and odd-mode propagation paths or equalizing phase velocities between these two modes [10]. However, these methodologies require design parameter recalculations or unrealistically tight fabrication tolerances. In several research studies, compact BPF structures have been proposed, but the design process is complicated because several parameters need to be considered [11,12].

In this paper, a miniaturized coupled-line resonator based on a doubly inductive compensation technique to raise the voltage coupling coefficient is proposed. Section II presents the concept of the inductively compensated resonator. The proposed resonators are applied to design a BPF. Examples of BPF designs based on the proposed resonators are presented, and their simulation and experiment results are discussed in Section III. The paper is finally concluded in Section IV.

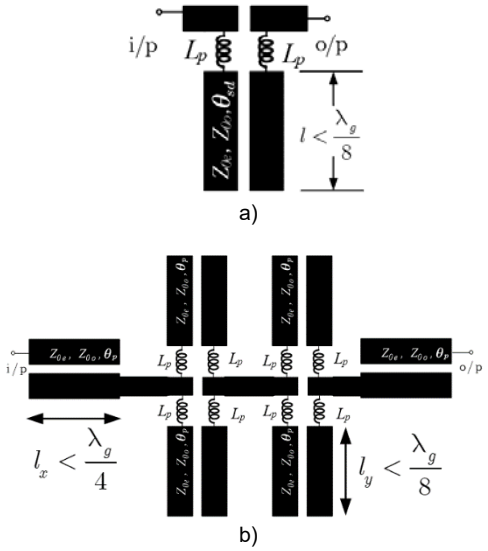

Fig.1. Schematics of the proposed resonators : (a) single-section BPF resonator-based inductively compensated octadic-wavelength coupled lines and (b) cascade-shunted BPF with coupled lines fed.

Proposed resonators

Basic resonator cell

The proposed resonator is developed based on an inductive compensation technique applied to parallel coupled lines. Fig. 1 shows the basic resonator cell, which consists of two compensated inductors connected with

parallel open-ended coupled lines. These two inductors connect at the input and the coupled ports of the coupled lines. The inductance, as shown in Fig. 1 (a), is optimally chosen such that a 90° phase difference between the input and coupled ports at the center frequency is obtained. Using network theory, we find that is computed from [13].

$$(1)\ L_{sd} = \frac{1}{2\pi f_0}\,\mathrm{Im}\left\{\frac{Z_{0o}\left(Z_{0c}^2 + Z_0^2\right)\sinh\theta_c - Z_{0c}\left(Z_{0o}^2 + Z_0^2\right)\sinh\theta_o - 2Z_0^3\Theta}{Z_0\left(Z_{0c}\sinh\theta_o + Z_{0o}\sinh\theta_c\right) - Z_0^2\Theta}\right\}$$

where: $\theta = \cosh\theta_e - \cosh\theta_o$ and $\Phi = \sqrt{\varepsilon_{effo}/\varepsilon_{effe}}$

Z_0 is the characteristic impedance of the coupled lines; Z_{0e} is the even-mode characteristic impedance of the coupled lines; Z_{0o} is the odd-mode characteristic impedance of the coupled lines; ε_{effe} is the even-mode effective dielectric constant; ε_{effo} is the odd-mode effective dielectric constant; $\theta_e = \pi/8$ is the even-mode electrical length of the coupled lines; $\theta_o = (\pi/8)\Phi$ is the odd-mode electrical length of the coupled lines.

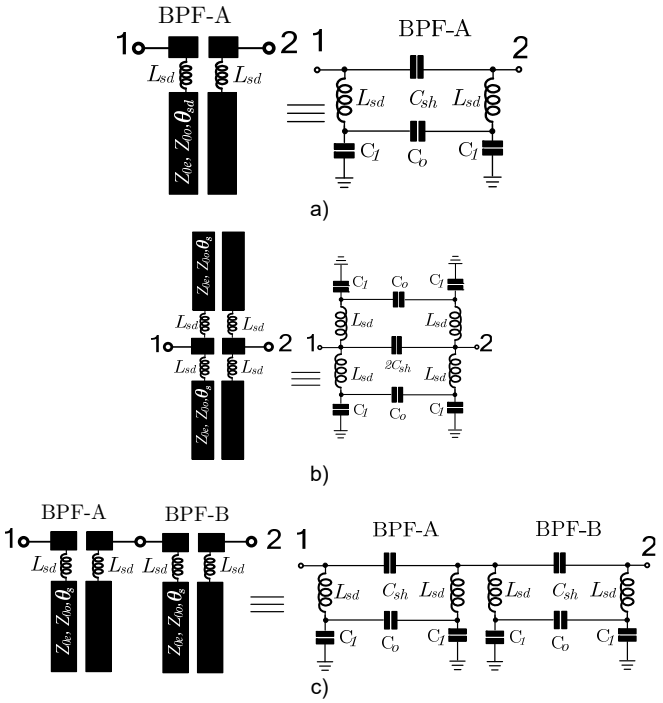

Fig.2. Schematics and equivalent circuits of the (a) single-section, (b) shunted and (c) cascaded resonators.

Fig. 2 (a) shows the diagram of a single-section resonator and its equivalent circuit. The compensation inductor (L_{sd}), if not large, can be implemented with a series transmission line. In the equivalent circuit, capacitors (C_{sh}) and (C_o) represent the coupling effect between the input and the coupled ports, while capacitor (C_1) represents open-ended lines. From the single-section resonator, we propose two topologies, as shown in Fig. 2 (b) and (c). Fig. 2 (b) and (c) show the shunt and cascaded topologies, respectively. The shunt topology is formed with two single-section resonators connected in parallel, whereas the cascade topology is formed with two single-section resonators connected in a cascade fashion. The equivalent circuits of both topologies are illustrated in Fig. 2 (b) and (c), and they are developed based on the equivalent circuit of the single-section resonator, as shown in Fig. 2 (a).

Design equations

Fig. 3 shows the diagram of the single-section resonator and its ports. The circuit operates under sinusoidal steady-state conditions. The upper compensated inductor connects to port 1 and the input port, whereas the lower one connects to port 2 and the coupled port. Ports 3 and 4 are the isolated and direct ports of the parallel coupled lines. With ports 3 and 4 open, port currents I3 and I4 are zero. Applying the 4-port impedance parameter, the relationship of the voltages and currents of each coupled-line port can be written as Equations (2)-(5):

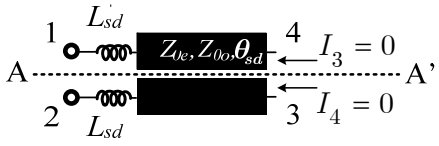

Fig.3. The proposed 2-port BPF resonator-based inductively compensated coupled lines.

$$(2)\quad V_1 = (Z_{11} + Z_{sd})I_1 + Z_{12}I_2 + Z_{13}I_3 + Z_{14}I_4$$

$$(3)\quad V_2 = Z_{21}I_1 + (Z_{22} + Z_{sd})I_2 + Z_{23}I_3 + Z_{24}I_4$$

$$(4)\quad V_3 = Z_{31}I_1 + Z_{32}I_2 + Z_{33}I_3 + Z_{34}I_4$$

$$(5)\quad V_4 = Z_{41}I_1 + Z_{42}I_2 + Z_{43}I_3 + Z_{44}I_4$$

where Vn and In (n= 1. 4) are the voltage and current at port n, respectively. Applying the condition, the 4-port network is then reduced to a 2 port network. This leads to the following:

$$(6)\quad \begin{bmatrix} V_1 \\ V_2 \end{bmatrix} = \begin{bmatrix} Z_{sd} + Z_{11} & Z_{12} \\ Z_{21} & Z_{sd} + Z_{22} \end{bmatrix}\begin{bmatrix} I_1 \\ I_2 \end{bmatrix} = \begin{bmatrix} Z_{11T} & Z_{12T} \\ Z_{21T} & Z_{22T} \end{bmatrix}\begin{bmatrix} I_1 \\ I_2 \end{bmatrix}$$

$$\begin{bmatrix} V_1 \\ V_2 \end{bmatrix} = \begin{bmatrix} Z_{sd} + Z_{11} & Z_{12} \\ Z_{21} & Z_{sd} + Z_{11} \end{bmatrix}\begin{bmatrix} I_1 \\ I_2 \end{bmatrix} = \begin{bmatrix} Z_{11T} & Z_{12} \\ Z_{12} & Z_{11T} \end{bmatrix}\begin{bmatrix} I_1 \\ I_2 \end{bmatrix}$$

Since the resonator is symmetrical along the AA' axis, as shown in Fig. 3, $Z_{11T} = Z_{22T} = Z_{sd} + Z_{11}$ and $Z_{sd} = j\omega L_{sd}$. The reflection coefficient at port 1 (S_{11}) and the forward transmission coefficient (S_{21}) of the single-section resonator are shown in (7) and (8), respectively [14]:

$$(7)\quad S_{11} = \frac{\left(Z_{11T}^2 - Z_0^2\right) - Z_{12}^2}{\left(Z_{11T} + Z_0\right)^2 - Z_{12}^2}$$

$$(8)\quad S_{21} = \frac{2Z_0Z_{12}}{\left(Z_{11T} + Z_0\right)^2 - Z_{12}^2}$$

where Z_0 is the system impedance. From Equations (2)-(5),

when $Z_{11} = \frac{1}{2}\left(Z_{0e}\coth(\theta_e) + Z_{0o}\coth(\theta_0)\right)$

and $Z_{12} = \frac{1}{2}\left(Z_{0e}\coth(\theta_e) - Z_{0o}\coth(\theta_0)\right)$

we substitute these relations into (7) and (8). Therefore, S_{11} and S_{21} of the single-section resonator will be simplified to

$$S_{11} = \frac{Z_{sd}^2 - Z_0^2 + \left(2Z_{sd}Z_{11} + Z_0^2 \coth(\theta_e)\coth(\theta_o)\right)}{\left(Z_{sd} + Z_0 + Z_{11}\right)^2 - {Z_{12}}^2} \quad (9)$$

$$S_{21} = \frac{2Z_0 Z_{12}}{\left(Z_{sd} + Z_0 + Z_{11}\right)^2 - {Z_{12}}^2} \quad (10)$$

By setting the electrical length of the coupled-line section to λ/8, the transmission responses (S_{21}) of the λ/8 single-section resonator for various coupling coefficients are investigated while the compensated inductor is computed from (1). In this paper, the voltage coupling coefficients were varied from -20 to -5 dB. Fig. 4 plots the magnitude of X_{Lsd} and θ_{sd} required for the design. It is shown that the required reactance increases as the voltage coupling coefficient increases. This contrasts with θ_{sd}, which decreases with the coupling coefficient. Applying X_{Lsd} and θ_{sd} to the single-section resonator, the magnitudes and phases of S_{21} of the resonators are plotted in Fig. 5 (a) and (b), respectively. The magnitude of S_{21} is raised at f_0, while the phase of S_{21} is 0 degrees at f_0. As shown in Fig. 5 (b), the slope of the S_{21} phase around f_0 depends on the voltage coupling coefficients. This means that the quality factor of the proposed resonator depends on the coupling coefficient.

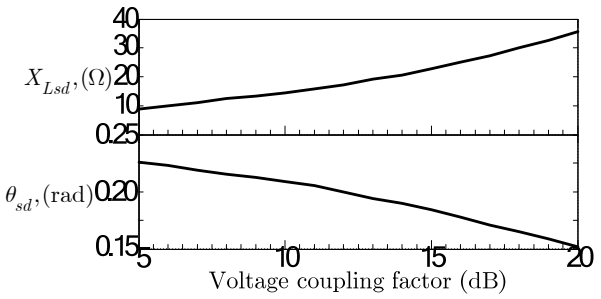

Fig.4. Magnitude of X_{Lsd} and θ_{sd}.

To verify the proposed technique, bandpass resonators operating at 1.57 GHz for a 50 Ω system were designed. A 10-dB coupled-line structure was chosen. For parallel coupled lines, we found that the even- and odd-mode impedances of the coupled lines were $Z_{0e1} = 69.37\ \Omega$ and $Z_{0o1} = 36.03\ \Omega$, respectively. In this study, four resonator circuits, which are a single-section resonator, a cascaded structure, a shunted structure and a mixed-mode structure, were investigated. Table I lists the electrical and physical parameters of the uncompensated and compensated one-section parallel coupled lines.

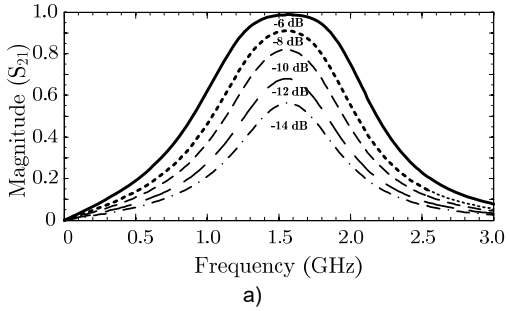

a)

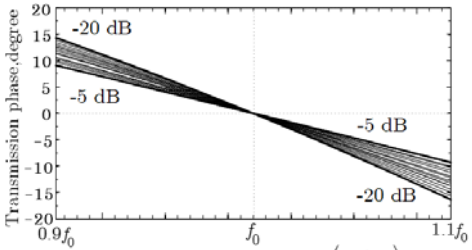

b)

Fig.5. Magnitude and phase (S_{21}) of the single-section resonator with a coupling factor from -20 to -5 dB.

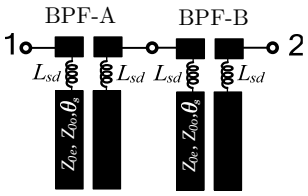

a)

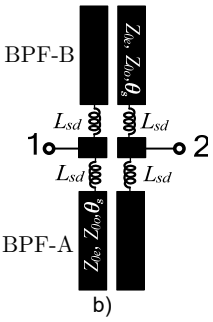

b)

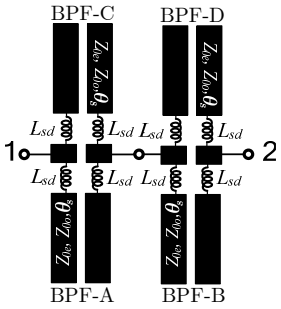

c)

Fig.6. Magnitude and phase (S_{21}) of the single-section resonator with a coupling factor from -20 to -5 dB.

Fig. 7 compares the simulated S_{21} responses of four resonators. Considering the cascaded and mixed-mode structures, the slopes around f_0 are steeper than those of the single-section and shunted structures. Based on these four resonators, three bandpass filters operating at 1.57 GHz were designed. The simulated S_{21} and the input return loss (S_{11}) are shown in Fig. 8(a) and Fig. 8(b). Quarter-wavelength (λ/4) parallel coupled lines were employed as input and output coupled fed lines. The simulated results show that the BPFs using the proposed resonators yield a passband at 1.57 GHz. A better than 20 dB return loss is obtained from four BPFs. Compared with the single-section and shunted-section structures, the cascaded and mixed-mode structures provide a good attenuation slope around f_0.

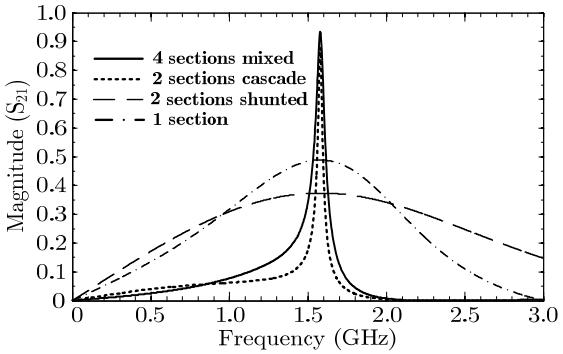

Fig.7. Frequency responses of the single-section resonator and the proposed BPF resonators shown in Fig. 6.

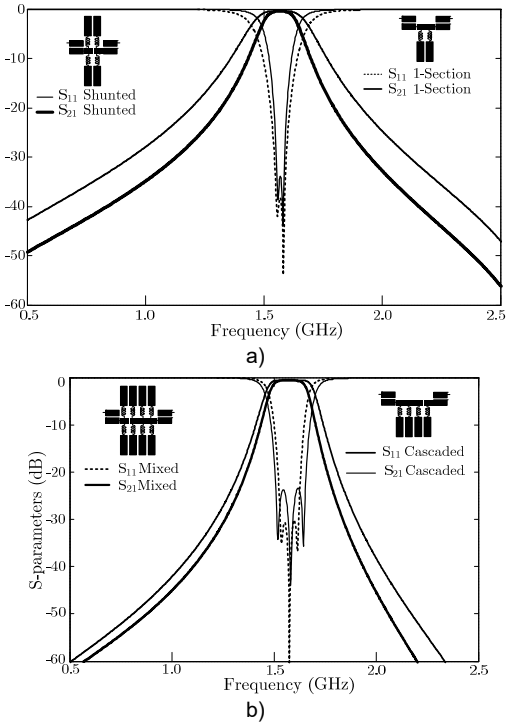

Fig.8. Simulated S_{21} and S_{11} of 4 BPF circuits based on (a) single-section and shunted structures (b) cascaded and mixed-mode structures.

Design and Experimental Results

To demonstrate the performance of the proposed technique, BPFs based on cascaded and mixed-mode structures were designed, fabricated and tested. A 10-dB coupled line was realized for the resonator. AD260 ($\varepsilon_r = 2.6,\ h$=1.0 mm, and $\tan\delta$=0.0017) were used for a printed circuit board. Based on the substrate parameters of AD260, we obtained $Z_{0e} = 69.37\ \Omega$, $Z_{0o} = 36.03\ \Omega$, and ε_{effe}=2.241, $\varepsilon_{effo} = 1.862$. Conventional coupled lines were used to design a BPF resonator. From (1) and (2), L_{sd} and θ_{sd} required 1.46 nH and 0.20π, respectively. Table II lists the electrical and physical parameters of the conventional BPF and the BPFs based on cascaded and mixed-mode structures. The electromagnetic simulation and measured results of the BPFs based on the proposed resonators and the conventional BPF are plotted in Fig. 9 and Fig. 10, respectively. The design and simulation process was performed using Sonnet Lite™. The measured results were obtained from an E5071C KEYSIGHT Technology network analyzer calibrated from 0.1 to 3 GHz. S_{21} and S_{11} at 1.57 GHz of these circuits are summarized in Table 3.

Table 1. Parameters of the designed one-section 1.57 GHz BPF resonator.

Techniques	Components	Coupler's length (θ,rad)	W, S, L (mm)
Uncompensated	-	0.25π	2.2, 0.17, 16.74
		0.50π	2.2, 0.17, 33.48
Compensated Inductors	L_{sd} = 1.46 nH	0.20π	2.2, 0.17, 13.39

Table 2. Parameters of the designed 2-section and 4-section 1.57 BPF resonators.

Techniques	Components	Coupler's length (θ,rad)	W, S, L (mm)
2-sections cascaded	L_{sd} = 1.46 nH	0.20π	2.2, 0.17,13.39
2-sections mixed	L_{sd} = 1.46 nH	0.20π	2.2, 0.17,13.39

Table 3. Parameters of the designed 2-section and 4-section 1.57 BPF resonators.

	2-sections cascaded	4-sections mixed cascade-shunted
S21(dB)	1.20	1.20
S11(dB)	23.20	21.80

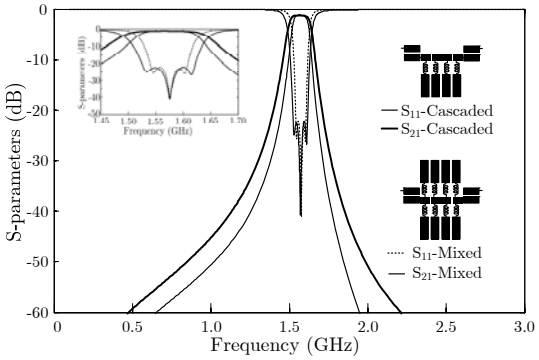

Fig.9. Comparison of EM simulated results between 2 cascaded sections and 4 mixed cascade-shunted sections of the proposed BPF-based doubly inductive compensated λ/8 coupled lines.

Fig. 8 and Fig. 9 show that the skirt slope in the transition bands depends on the number of BPF resonator sections. The proposed technique achieves less than 1.20 dB insertion loss (S_{21}) and less than 24.80 dB return loss (S_{11}) performance at passband frequencies, as shown in Fig. 10. Moreover, the suppression performance at twice the harmonic frequency $2f_0$ is more than 55 dB. The PCB photographs of the proposed 2-section cascaded and 4-section mixed cascade-shunted BPF circuits are shown in Fig. 11(a) and (b), respectively. The sizes of the 2-section cascaded and 4-section mixed cascade-shunted BPF circuits are 27×78 mm^2 and 48×78 mm^2, which are approximately 54% and 95% of the size of the conventional design of the 3rd-order microstrip parallel coupled lines BPF (27×145 mm^2), respectively.

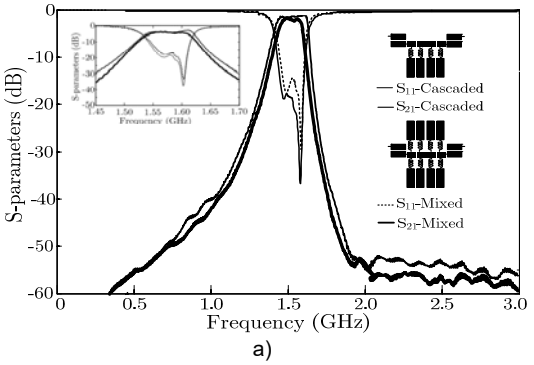

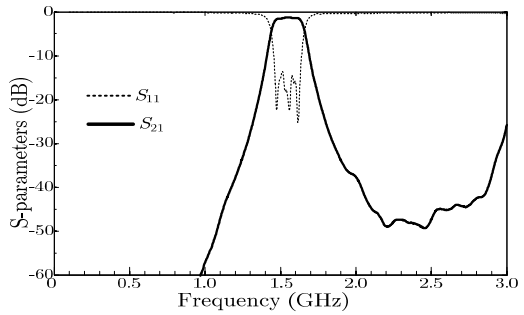

b)

Fig.10. Comparison of measured results between (a) 2-section cascaded and 4-section mixed cascade-shunted of the proposed BPF and (b) the 3rd-order microstrip parallel coupled lines BPF.

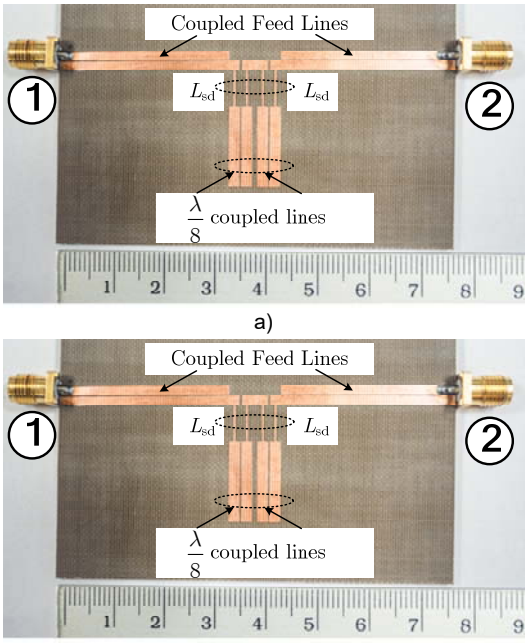

a)

b)

Fig.11. Comparison of measured results between (a) 2-section cascaded and 4-section mixed cascade-shunted of the proposed BPF and (b) the 3rd-order microstrip parallel coupled lines BPF.

Conclusion

Based on the simple inductive compensation technique, we have presented a new method to miniaturize the circuit size of microstrip BPF-based coupled lines by replacing ordinary quarter-wavelength coupled lines with the proposed inductively compensation octadic-wavelength coupled lines in microstrip circuits. The proposed filters exhibit higher suppression performance than the filter-based ordinary coupled lines. Additionally, the design procedures are convenient due to the available closed-form design equations. The compensating inductors are connected in series with the input and coupled ports of the octadic-wavelength coupled lines with the appropriate shortened length for adjusting the 90° phase difference between the input and coupled ports of the BPF resonator at a center frequency of f_0. The measured results obtained from the proposed BPF exhibit less than 1.20 dB insertion (S_{21}), 23.20 dB return losses (S_{11}) and more suppression performance than 55 dB at twice the harmonic frequency 3.14 GHz. The proposed BPF provides a steep skirt slope with a compact size. The optimum value of the compensation inductor is relatively small, so the technique can be practically implemented in microwave and millimeter-wave applications. The design procedures for these circuits with the compensation technique are described. The design task is simplified by closed-form expressions for determining the compensation inductor values and coupled-line parameters. Since there are various microwave communication circuits whose structures consist of parallel coupled lines, it is believed that the technique is highly applicable and suitable for modern wireless communications.

Acknowledgments

This work is financially supported by the Department of Computer and Communication Engineering Faculty of Technology, Udon Thani Rajabhat University. We thank you Mr. Somkuan Srisawat for AD260A substrate.

***Authors**: Asst. prof. dr Ravee Phromloungsri, Department of Computer and Communication Engineering, Faculty of Technology, Udon Thani Rajabhat University, Udon Thani, Thailand, E-mail: phravee@gmail.com ; Prof. dr Mitchai CHONGCHEAWCHAMNAN, Faculty of Engineering, Prince of Songkla University, Hat Yai Songkla, Thailand, E-mail: mitchai@coe.psu.ac.th; Asst prof. dr Somchat SONASANG, Department of Electronic Technology, Faculty of Industrial Technology, Nakhon Phanom University, Nakhon Phanom, Thailand, E-mail: somchat.s@npu.ac.th*

REFERENCES

[1] G. L. Matthaei, L. Yolig, and E.M.T Jones, Microwave Impedance-Matching Network and Coupling Structures, New York: McGraw-Hill, 1964, pp.583-593.

[2] S. Jovanovic, A. Nesic, “Microstrip bandpass filter with a new type of capacitive coupled resonators”, Electronics Letters, Vol. 41, No. 1, January 2005.

[3] J.T. Kuo, E. Shoh, “Microstrip Stepped Impedance Resonator Bandpass Filter With an Extended Optimal Rejection Bandwidth”, IEEE Transactions on Microwave Theory and Techniques, Vol.51, No. 15, May 2003.

[4] C-M. Tsai, S-Y Lee, H-M Lee, “Transmission-Line Filters with Capacitively Loaded Coupled Lines”, IEEE Transactions on Microwave Theory and Techniques, Vol. 51, No. 15, May 2003.

[5] J. S. Hong, and M. J. Langcaster, “Theory and experiment of novel microstrip slow-wave open-loop resonator filter”, IEEE Trans. Microwave Theory Tech., vol. 45, no.12, 2006, pp. 2358-2365.

[6] T. Edward, Foundation for Microstrip Circuit Design, West Sussex, England: John Wiley & Son, 1992, pp. 173-228.

[7] I. J. Bahl, “Capacitively compensated performance parallel coupled microstrip filter”, in 1989 IEEE MTT-S Int. Microwave Symp. Dig., June 1989, pp. 679-682.

[8] R. Phromloungsri, M. Chongcheawchamnan, and I. D. Robertson, “Inductively compensated parallel coupled microstrip lines and their applications”, IEEE Trans. Microwave Theory Tech., vol. 54, no.9, pp. 3571-3582, Sept. 2006.

[9] T. C. Edwards and M. B. Steer, "Applications of Parallel-coupled Microstrip Lines," in Foundations for Microstrip Circuit Design, IEEE, 2016, pp.306-338.

[10] A. Riddle, "High performance parallel coupled microstrip filters," 1988., IEEE MTT-S International Microwave Symposium Digest, 1988, vol.1, pp. 427-430.

[11] C. H. Wu, Y. S. Lin, C. H. Wang and C. H. Chen, "Compact microstrip coupled-line bandpass filter with four transmission zeros," in IEEE Microwave and Wireless Components Letters, vol. 15, no. 9, 2005, pp. 579-581.

[12] T. K. Das and S. Chatterjee, "Harmonic Suppression in a Folded Hairpin-Line Cross-Coupled Bandpass Filter by using Spur-Line," 2021 Devices for Integrated Circuit (DevIC), 2021, pp. 474-478.

[13] N. Thammawongsa, R. Phromloungsri, M. Jamsai, and N. Pornsuwancharoen, “Design elliptic lowpass filter with inductively compensated parallel-coupled lines”.in Procedia Eng. 2012, 32, 550–555.

[14] L. Zhu, S. Sun, and R. Li “Microwave Bandpass Filters for Wideband Communications”, John Wiley & Sons, Inc., 2012, New York.

[15] S. Kumpang, R. Phromloungsri, M. Chongcheawchamnan, and M. Krairiksh, “Design and application of microstrip parallelcoupled lines employing step-impedance transmission-line compensation”, IET Microw. Antennas Propag., vol. 3, Issue 3, pp. 410-415, April, 2009.